

## Drag reduction strategies

By D. C. Hill

### 1. Motivation and objectives

In last year's Annual Research Briefs (Hill 1993) a description was given of an active control scheme using wall transpiration that leads to a 15% reduction in surface skin friction beneath a turbulent boundary layer, according to direct numerical simulation. In this research brief further details of that scheme and its variants are given together with some suggestions as to how sensor/actuator arrays could be configured to reduce surface drag. The research which is summarized here was performed during the first half of 1994.

This research is motivated by the need to understand better how the dynamics of near-wall turbulent flow can be modified so that skin friction is reduced. The reduction of turbulent skin friction is highly desirable in many engineering applications. Experiments and direct numerical simulations have led to an increased understanding of the cycle of turbulence production and transport in the boundary layer (Robinson 1991) and raised awareness of the possibility of disrupting the process with a subsequent reduction in turbulent skin friction (Bushnell & McGinley 1989, Blackwelder 1989). The implementation of active feedback control in a computational setting is a viable approach for the investigation of the modifications to the flow physics that can be achieved (Choi *et al.* 1994).

Bewley *et al.* (1993) and Hill (1993) describe how ideas from optimal control theory are employed to give "sub-optimal" drag reduction schemes. The objectives of the work reported here is to investigate in greater detail the assumptions implicit within such schemes and their limitations. It is also our objective to describe how an array of sensors and actuators could be arranged and interconnected to form a "smart" surface which has low skin friction.

### 2. Accomplishments

As before, the various schemes are aimed at reducing the mean drag upon a plane wall by the application of distributed or localized blowing and suction. There is no net mass flux through the wall, and an expense is associated with the control action. The simulations are performed for a channel flow with a constant mass flux through the channel. The Reynolds number based on friction velocity is of the order 100 for the tests.

#### 2.1 Assumptions

The sub-optimal drag reduction scheme of Hill (1993) is based upon minimizing the drag by considering how the flow is most favorably influenced during consecutive short time intervals. In order to arrive at the relatively simple control law, several assumptions must be made about the flow field.

Only flow structures in a layer close to the wall are significant in deciding how control will modify the flow evolution. The characteristic thickness of this *layer of influence* is

$$L_T = \frac{4}{3} \sqrt{\frac{T}{\pi}} \text{ wall units,} \quad (1)$$

where  $T$  is the *control time interval* in wall units over which the local optimization is made. The layer of fluid between the wall and  $y^+ = L_T$  will be referred to as the layer of influence. The dynamics of the flow within this layer guides the control force distribution.

One concern about the original derivation of the result reported last year was the assumption that there is no mean shear at the wall. The flow was taken to be uniform, and the effects of mean shear were assumed to be negligible. Following a considerable analytical effort, that assumption has been shown to be valid. A re-derivation of the scheme with mean shear effects included leads to the same result as that presented by Hill (1993).

Other assumptions made during the derivation have been clarified:

1. *Events far from the surface are not modified significantly by the effect of the surface control velocities.*

2. *On the control time interval, mixing within the layer of influence is sufficiently weak that it plays a negligible role in the transport of control signals.* There is an unsteady component in the near-wall flow field. The effect of unsteadiness in transporting the control signals has been neglected. Note that this does not mean that unsteadiness has been neglected.

3. *Those flow structures which govern the sensitivity of the immediate drag to changes in the control distribution do not evolve significantly on the control time interval.*

4. *The layer of influence is sufficiently thin that the mean and unsteady flow components within the layer are represented well by a low order Taylor expansion at the wall.* It is assumed that the differential scale in the wall-normal direction of the velocity fluctuations is much larger than the thickness of the layer of influence.

It is important to recognize that the present control theory deals only with efficient changes to the behavior of the viscous sub-layer region. The physics of the sweep events and turbulence production involves events further from the wall which have a much longer time scale than that of the optimization. Consequently, these flow characteristics are not necessarily modified in an optimal manner. They are influenced indirectly by the modifications which are applied in the viscous sub-layer.

## 2.2 Variants of the original scheme

Using the sensitivity function, two classes of scheme have been devised and tested by direct numerical simulation. The wall-normal velocity component at the  $n$ th time step is represented by its Fourier transform,  $\hat{\Phi}^{(n)}(\alpha, \beta)$ , where  $\alpha$  and  $\beta$  are

streamwise and spanwise wave numbers ( $\gamma = \sqrt{\alpha^2 + \beta^2}$ ). The Fourier transform of the streamwise velocity fluctuations is denoted by  $\hat{u}^{(n)}(\alpha, \beta; y)$ .

1. In the spirit of Choi *et al.* (1994), we considered the scheme

$$\hat{\Phi}^{(n+1)}(\alpha, \beta) = \frac{\hat{u}^{(n)}(\alpha, \beta; L_T)}{(\ell - \frac{i\alpha}{2\gamma}(1 - \gamma L_T))}. \quad (2)$$

This scheme uses information within the flow domain at  $y^+ = L_T$ . With  $\ell = 1$  and  $L_T = 10$ , a drag reduction of 19% is achieved. The similar scheme of Choi *et al.*, which applies wall transpiration equal and opposite to the wall-normal velocity component at  $y^+ = 10$ , gives a reduction of about 23%.

2. The following relaxation scheme has been tried:

$$\hat{\Phi}^{(n+1)}(\alpha, \beta) = \frac{1}{1 + \mu(\ell - \frac{i\alpha}{2\gamma}(1 - \gamma L_T))} \left\{ \hat{\Phi}^{(n)}(\alpha, \beta) + \mu L_T \left( \frac{\partial \hat{u}^{(n)}}{\partial y} \right)_{y=0} \right\}, \quad (3)$$

where  $\mu$  is a relaxation parameter. This scheme uses wall information only and leads to a drag reduction of about 14% ( $\mu = 0.05, \ell = 1, L_T = 5$ ).

### 2.3 Implications for sensor and actuator arrays

In practice an active drag reduction system is likely to consist of an array of wall-mounted sensors and actuators. For the present scheme, the sensors must measure the streamwise component of wall shear, while the ‘‘actuators’’ are orifices through which fluid is injected and removed. The control velocity at a particular actuator is updated on the basis of information from the sensors in its neighborhood. The prior control velocities at neighboring actuators are also required.

Consider a rectangular array of locations on the wall at which the control velocity is specified. Variable  $\Phi_{i,j}^{(n)}$  denotes the control velocity at the  $i$ th streamwise and  $j$ th spanwise position. Let  $h_x^a$  and  $h_z^a$  be the streamwise and spanwise spacing, respectively, between actuators. Suppose that the unsteady component of wall shear in the streamwise direction,  $\sigma_{i,j}^{(n)}$ , is measured at a similar array of sensor positions, which is offset from the actuator array. Let  $h_x^s$  and  $h_z^s$  be the streamwise and spanwise spacing of the sensors. In order to define the control update at the  $(i, j)$ th actuator, data from a number of neighboring actuators and sensors is employed. Let there be  $N_x^a$  streamwise and  $N_z^a$  spanwise actuators and  $N_x^s$  streamwise and  $N_z^s$  spanwise sensors.

The following scheme is proposed:

$$\Phi_{i,j}^{(n+1)} = \sum_{k=1}^{N_x^a} \sum_{l=1}^{N_z^a} W_{k,l}^a \Phi_{i+k,j+l}^{(n)} + \mu L_T \sum_{k=1}^{N_x^s} \sum_{l=1}^{N_z^s} W_{k,l}^s \sigma_{i+k,j+l}^{(n)}. \quad (4)$$

The weights are

$$\begin{aligned} W_{k,l}^a &= c(k, N_x^a) c(l, N_z^a) h_x^a h_z^a K(-x_{k,l}^a, -z_{k,l}^a), \\ W_{k,l}^s &= c(k, N_x^s) c(l, N_z^s) h_x^s h_z^s K(-x_{k,l}^s, -z_{k,l}^s), \\ c(k, N) &= 1/2, \text{ if } k = 1, N, \\ &= 1 \text{ otherwise,} \end{aligned} \quad (5)$$

where  $(x_{k,l}^a, z_{k,l}^a)$  and  $(x_{k,l}^s, z_{k,l}^s)$  are the locations of the actuators and sensors, respectively, measured relative to the location of the actuator for which the control velocity is being computed.

The function  $K(x, z)$  is defined by

$$K(x, z) = \frac{1}{4\pi^2} \int_{-\alpha_0}^{\alpha_0} \int_{-\beta_0}^{\beta_0} \frac{e^{i(\alpha x + \beta z)}}{(1 + \mu(\ell - \frac{i\alpha}{2\gamma}(1 - \gamma L_T)))} d\beta d\alpha. \quad (6)$$

The wave number cutoffs  $\alpha_0$  and  $\beta_0$  are introduced since the derivation for the analytical control law is not defined as  $\alpha$  and  $\beta$  become very large. Preliminary experience suggests that the application of this cutoff does not have a detrimental effect.

It has been found that only a few neighboring points offer a significant contribution to the summation; the weight factors  $W_{i,j}^{a,s}$  diminish rapidly in magnitude as  $|i|$  and  $|j|$  are increased. This is very encouraging since it suggests that a control stencil that employs information from nearby sensors and actuators alone may be quite effective. Experience with the spectral version of the control scheme suggests that the streamwise spacing between actuators/sensors should not exceed 12 wall units if the scheme is to be effective. The spanwise spacing should not exceed 4 wall units.

Once more the author is indebted to T. Bewley for his time, patience, and effort in the implementation of these rules in the direct numerical simulations.

#### REFERENCES

- BEWLEY, T., CHOI, H., TEMAM, R. & MOIN, P. 1993 Optimal feedback control of turbulent channel flow. *Annual Research Briefs-1993*. Center for Turbulence Research, NASA-Ames/Stanford Univ.
- BLACKWELDER, R. F. 1989 Some ideas on the control of near-wall eddies. *AIAA Paper No. 89-1009*.
- BUSHNELL, D. M., & MCGINLEY, C. B. 1989 Turbulence control in wall flows. *Ann. Rev. Fluid Mech.* **21**, 1-20.
- CHOI, H., MOIN, P., & KIM, J. 1994 Active turbulence control for drag reduction in wall-bounded flows. *J. Fluid Mech.* **262**, 75-110.
- HILL, D. C. 1993 Drag reduction at a plane wall. *Annual Research Briefs-1993*. Center for Turbulence Research, NASA Ames/Stanford Univ.
- ROBINSON, S. K. 1991 Coherent motions in the turbulent boundary layer. *Ann. Rev. Fluid Mech.* **23**, 601-639.

# Optimal active control for Burgers equation

By Yutaka Ikeda<sup>1</sup>

A method for active fluid flow control based on control theory is discussed. Dynamic programming and fixed point successive approximations are used to accommodate the nonlinear control problem. The long-term goal of this project is to establish an effective method applicable to complex flows such as turbulence and jets. However, in this report, the method is applied to stochastic Burgers equation as an intermediate step towards this goal. Numerical results are compared with those obtained by gradient search methods.

## 1. Motivation and objectives

There is current research at Stanford to develop active feedback control schemes based on optimal control theory to control turbulence. In particular, an optimal control method based on a gradient search algorithm is discussed in Choi, Teman and Moin (1993) and Bewley and Moin (1994). Such gradient schemes, however, are not guaranteed to converge to the global minimum of the cost functional and thus may suffer from degraded performance when compared with the "optimal" in a given situation.

The objective of the current research is to investigate an alternative method to the gradient search method without increasing computational complexity. The approach we take is to impose the convexity onto the cost functional and derive the analytical optimal controlled solutions for a set of linearized systems. This eliminates the minimization process of the cost functional. Then the optimal controlled solution for stochastic Burgers equation is found by Fixed Point Theorem. The resulting method is compared with the gradient method through numerical simulation, then assessments for applicability to more complex flow dynamics are made.

## 2. Scheme for optimal control

### 2.1 System model

We consider stochastic Burgers equation as a system model:

$$\frac{\partial u}{\partial t} = \frac{1}{Re} \frac{\partial^2 u}{\partial x^2} - \frac{\partial}{\partial x} \frac{u^2}{2} + F + \chi. \quad (1)$$

Initial condition and boundary conditions are given by  $u(x, t_0) = u_0(x)$ ,  $x \in (0, 1)$  and  $u(0, t) = u(1, t) = 0$ ,  $t \in [t_0, T]$ . Also,  $Re$ ,  $F(x, t)$ , and  $\chi(x, t)$  denote Reynolds number, a forcing term, and a normally distributed random forcing term with zero mean and unit variance, respectively.

<sup>1</sup> McDonnell Douglas Aerospace

In order to control the velocity gradient  $v = \partial u / \partial x$ , we introduce the dynamics of the velocity gradient, which can be formally obtained by differentiating Burgers equation with respect to  $x$  such that

$$\frac{\partial v}{\partial t} = \frac{1}{Re} \frac{\partial^2 v}{\partial x^2} - u \frac{\partial v}{\partial x} - u_x v + f + \xi \quad (2)$$

where  $f(x, t) = \partial F(x, t) / \partial x$  denotes the control forcing term for the differential form of Burgers equation and  $\xi = \partial \chi(x, t) / \partial x$ , a formally differentiated random forcing term.

### 2.2 Cost functional

We consider a control problem in which the cost functional to be minimized is given by

$$J = \frac{1}{2} E \left[ \int_{t_0}^T \int_0^1 (m_d \left( \frac{\partial u}{\partial x} \right)^2 + l_d (f(x, t))^2) dx dt \right], \quad (3)$$

where  $E[\cdot]$  denotes a mathematical expectation. In a more general setting, the state, control, and the cost functional can be formed by

$$X = \begin{pmatrix} u \\ \frac{\partial u}{\partial x} \end{pmatrix}, \quad U = \begin{pmatrix} F \\ f \end{pmatrix},$$

and

$$J = \frac{1}{2} E \left[ \int_{t_0}^T \int_0^1 (m_d (X^T Q X) + l_d (U^T R U)) dx dt \right], \quad (4)$$

where

$$Q = \begin{pmatrix} q_1 & 0 \\ 0 & q_2 \end{pmatrix} \quad \text{and} \quad R = \begin{pmatrix} r_1 & 0 \\ 0 & r_2 \end{pmatrix}.$$

If we select  $q_1$  small relative to  $q_2$  and  $r_2$  small relative to  $r_1$ , we can formulate a problem similar to that discussed in Choi *et al.* (1993). However, this introduces a higher dimension of the system dynamics. For computational simplicity, control of the decoupled (1-D) system rather than the augmented (2-D) system is considered by selecting  $q_1 = r_1 = 0$ , which results in (3).

### 2.3 Optimal control strategy

A brief summary of the optimal control strategy is now given:

\* *Linearize system:* Consider the system given by the linear equation

$$\frac{\partial v}{\partial t} = \frac{1}{Re} \frac{\partial^2 v}{\partial x^2} - u_{opt} \frac{\partial v}{\partial x} - (u_{opt})_x v + f + \xi, \quad (5)$$

where  $u_{opt}$  denotes the solution of Burgers equation (1) when the optimal control  $f_{opt}$  is applied to the system (2).

- \* *Design a linear optimal controller:* The dynamic programming technique is applied to the linear distributed parameter system (5) to find the optimal control for the linear system (for detail, see Tzafestas and Nightingale 1968).
- \* *Compute optimal controlled solution  $u_{opt}$ :* Once the optimal controller for (5) is found, integrate Eq. (5) with respect to  $x$  to yield:

$$\frac{\partial u}{\partial t} = \frac{1}{Re} \frac{\partial^2 u}{\partial x^2} - u_{opt} \frac{\partial u}{\partial x} + F + \chi. \quad (6)$$

To solve (6) for the optimal controlled solution, we need to know the optimal solution before it is solved. Hence, for the moment, we replace  $u_{opt}$  in (5) and (6) by a known function  $w(x, t)$  and consider a mapping  $G(w)$  defined on a function space which maps  $w(x, t)$  to the solution  $u(x, t)$  of (6). Notice that for each  $w$  the optimal controller is designed for the linearized system, and thus each image  $u$  of  $G(w)$  forms an optimal solution for the corresponding system. Now, consider a family of optimal controlled solutions generated by  $G(w)$ . Then it is clear that the fixed point of  $G(w)$  (if it exists) is the optimal controlled solution  $u_{opt}$  of Burgers equation (6). To find the fixed point of  $G(w)$ , a method of successive approximations is employed.

### 3. Numerical simulation

An early evaluation of this new optimal control formulation is important for determining the promise of the approach. To accomplish this, an evaluation through comparison is performed between the current method and the gradient method investigated by Choi *et al.* A numerical example was taken from Choi *et al.* (1993) for a comparison study (distributed control problem, case(ii), where the weights  $l_d = 1$  and  $m_d = 1/dx$  in the cost functional,  $Re = 1500$  and  $dx = 2047$ ). However, only qualitative comparison is meaningful in the current comparison study since the control problem is set up differently from the gradient method by Choi *et al.* in order to keep the computational complexity low. That is, the current method uses the cost functional (3) as one of the simplest cases of the more general form (4) (see discussion in 2.2), while the gradient method by Choi *et al.* uses the integrated control  $F$  instead of  $f$  in the cost functional (3). Another difference is that the cost functional in Choi *et al.* (1993) is formulated without the integral sign with respect to time; hence, the cost is minimized at each instance of time rather than over a duration of time.

Two different values for the ratio  $l_d/m_d$  were considered. Case-1: the weights  $l_d$  and  $m_d$  were set to be identical with those in the example. Case-2: the weight  $l_d$  was reduced by a factor of 1000 to allow more control power, keeping the weight  $m_d$  the same. In each case, the time histories of the cost functional, control power used, and gradient at the wall ( $x = 0$ ) were computed. The results are shown in Figs. 1-3. The velocities at time 2 second are shown in Fig. 4. The corresponding figures from Choi *et al.* (1993) are also shown in Figs. 1, 2, and 4 for comparison.

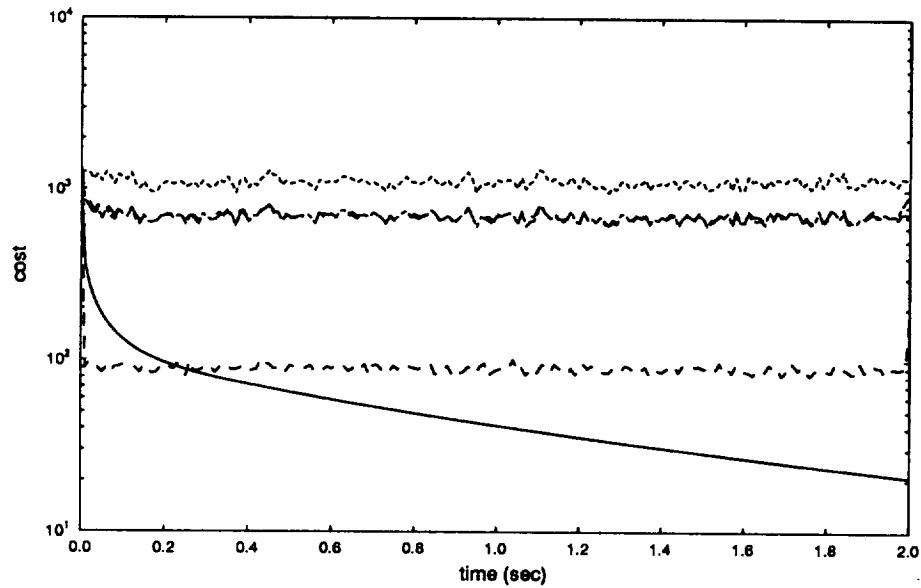


FIGURE 1. Time history of the cost functional. Legend: — , without forcing; ---- , with random forcing and no control; - - - , with control and random forcing (case 1); . . . , with control and random forcing (case 2); — — , with control and random forcing (Choi *et. al.*).

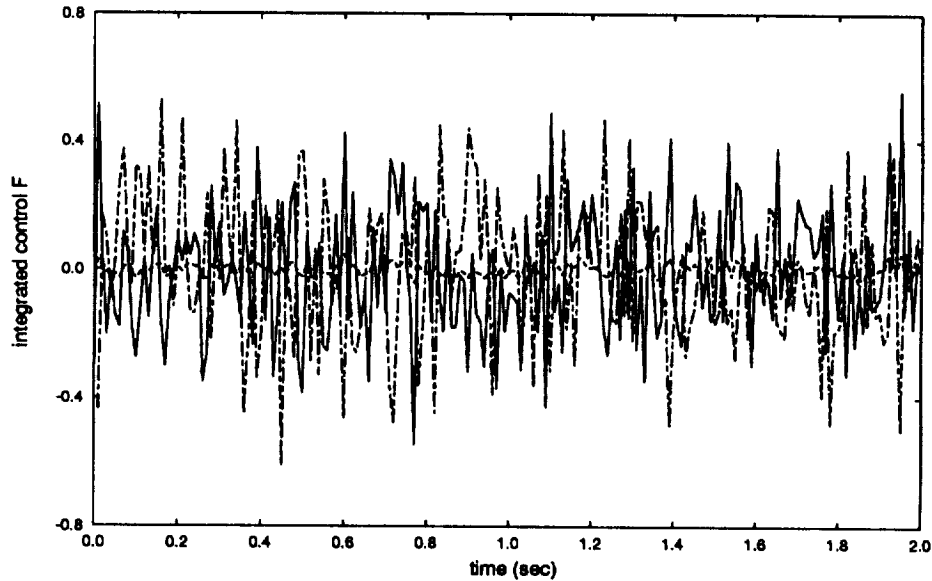


FIGURE 2. Time history of momentum forcing. Legend: — , control forcing (case 2); ---- , control forcing (case 1); - - - , control forcing (Choi *et. al.*).

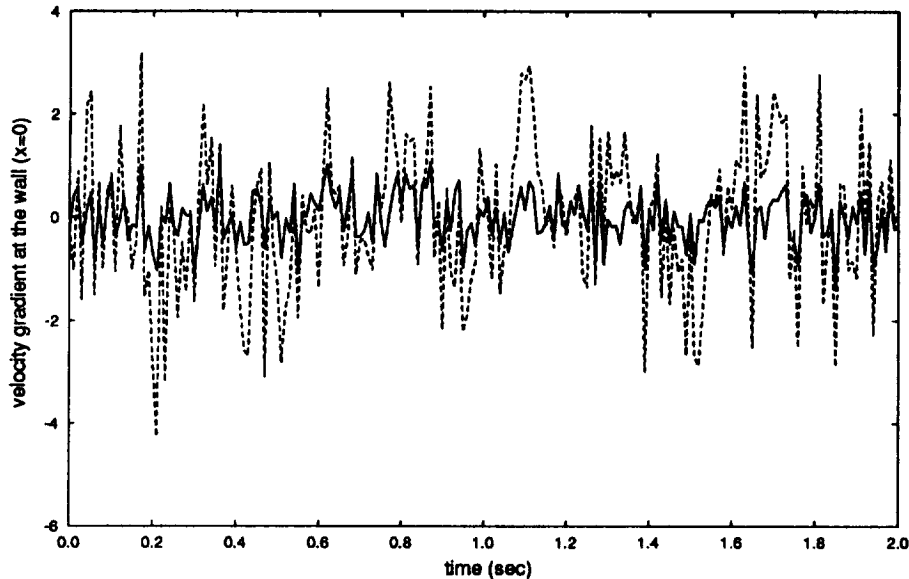


FIGURE 3. Wall velocity gradient at  $x = 0$ . Legend: —, with control and random forcing (case 2); ----, without control.

Fig. 1 shows that both methods reduced the cost functional significantly. The integrated control power  $F$  in each case of the current method and the gradient method are shown in Fig. 2. It shows that the amount of control  $F$  used in Case-1 is much less than that in Case-2 and the gradient method. Therefore, Case-2 seems more comparable to the example with the gradient method with respect to the momentum forcing added to Burgers equation. This seems natural since the velocity gradient becomes large in magnitude, particularly when the random noise is present. Hence, it requires more control power  $f$  when the velocity gradient is fed back than when the velocity is fed back. Fig. 3 shows that the current method controls the velocity gradient effectively if enough control power is allowed. Both Case-1 and the gradient method needed more control power to reduce the gradient at the wall significantly. From Fig. 4 it can be seen that the current method reduced the velocity magnitude as well as the velocity gradient while the gradient method did not reduce the velocity magnitude as much. This may be explained as follows: the current method seems to control the velocity gradient by regulating the gradient magnitude uniformly. Then, since the velocity at the boundaries are fixed to be zero, the velocity magnitude becomes small. On the other hand, the gradient method seems to control the velocity gradient by linearly scaling down. Hence, it reduces the absolute magnitude of the higher velocity gradient more significantly. One final observation is that the control formulated by the current method seems to respond more than a one order of magnitude faster than that by the gradient method (see Case-2 in Fig. 1, and Fig. 7(b) in Choi *et al.* 1993). This is a very important advantage for non-stationary applications.

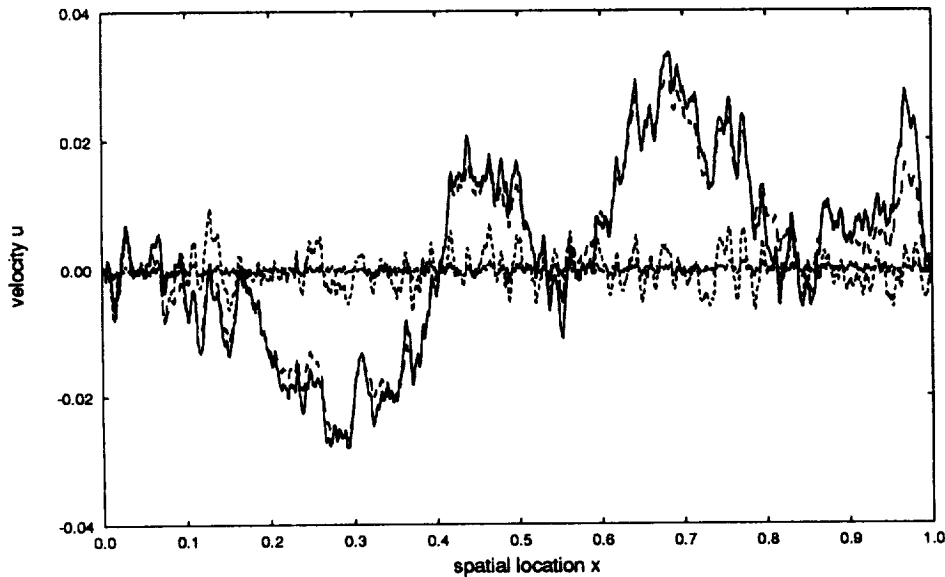


FIGURE 4. Velocity at  $t = 2$ . Legend: —, with random forcing and no control; ----, with random forcing and control (case 1); - · - ·, with random forcing and control (case 2); · · · ·, with random forcing and control (Choi *et. al.*).

#### 4. Conclusions

A method for active control of fluid flow dynamics was discussed. The simulation results show that the current control method works effectively and seems to be extendable to Navier-Stokes equations without major problems. Applications to turbulence and/or jet control will be attempted in the near future.

#### Acknowledgements

The author would like to acknowledge the financial support of McDonnell Douglas Corporation. The author also wishes to acknowledge Prof. Parviz Moin and Mr. Thomas Bewley for their helpful discussions and warm hospitality during the author's stay at CTR, and Prof. Hacheon Choi for providing useful information about the gradient method.

#### REFERENCES

- BEWLEY, T., & MOIN, P. 1994 Optimal control of turbulent channel flows. *ASME Winter Annual Meeting*, Chicago, 9 Nov. 94.
- CHOI, H., TEMAM, R., MOIN, P., & KIM, J. 1993 Feedback control for unsteady flow and its application to the stochastic Burgers equation. *J. Fluid Mech.* **253**, 509.
- TZAFESTAS, S., & NIGHTINGALE, J. 1968 Optimal control of a class of linear stochastic distributed-parameter systems. *Proc. IEE.* **115** (8), 1213, 1220.